AztABCD Zinc Transporter System

Zinc is an essential trace nutrient. In bacteria, its import into the cell is largely mediated by ATP binding cassette (ABC) transporters, which rely on extracellular solute binding proteins (SBP) to bind the metal with high affinity and specificity. In some cases, the SBPs work with other extracellular zinc binding proteins known as metallochaperones. The mechanisms of zinc transport in these systems is of interest because zinc ABC transporters have been shown to be essential for virulence in a number of pathogenic bacteria. This entry describes several structural features of a zinc SBP and related metallochaperone and their role in zinc binding and transfer.

1. Introduction

Transition metals such as zinc, iron, manganese, and copper provide essential cellular functions, yet are highly toxic in their "free" forms or bound to incorrect targets. Thus, all living things must carefully maintain metal homeostasis. In general, this is accomplished by regulating the uptake and efflux of metals from the cell as well as by proteins that bind, store, and/or shuttle metals to their appropriate destinations. Proteins of the latter description are known as metallochaperones. Well-studied examples include the Atox1, CCS, and Cox17 metallochaperones that deliver copper to specific targets in eukaryotes [1], and the metallothioneins that buffer zinc concentration in eukaryotes [2] and a few bacteria [3]. A new family of intracellular zinc-binding GTPases called COG0523 has been identified in bacteria. These are often upregulated by zinc starvation [4][5][6] and may function as metallochaperones. However, direct evidence of metal transfer to target proteins has never been demonstrated, and their physiological functions are often unclear.

Metal binding proteins outside the cell are also important for bacterial metal homeostasis. ATP binding cassette (ABC) transporters are critical for high affinity uptake of transition metals and other nutrients. In addition to dimeric membrane permease and cytosolic ATPase proteins, bacterial ABC transporters rely on periplasmic (Gram-negative) or cell surface (Gram-positive) solute binding proteins (SBP) [7][8]. The SBP is essential to bind the substrate with high affinity and specificity and deliver it to the membrane permease for transport into the cell. SBPs have been categorized according to structure and substrate specificity [9], with members of group A-I mediating transport of zinc, manganese, or iron. The presence of a flexible loop rich in His/Asp/Glu residues near the metal binding site is indicative of zinc specificity [10]. These proteins have garnered considerable interest as potential antibiotic targets as they are required for high affinity zinc import and survival under the extremely zinc-limited conditions imposed by animal hosts [11][12].

The cluster A-I SBPs are not the only extracellular bacterial zinc metallochaperones. In a surprising number of cases, metal may be transferred to them by other metallochaperones. Examples of such chaperones include ZinT [13][14][15][16][17][18][19], the polyhistidine triad protein PhtD [20][21][22], and AztD [23]. Direct zinc transfer to an SBP has only been demonstrated for the latter two, and the mechanistic details of this process are unclear. This is typically the case despite the importance of zinc transfer processes in biology due to the lack of a convenient spectroscopic handle for this element. However, the kinetics of transfer from AztD to AztC can be easily followed by a roughly 2-fold increase in intrinsic protein fluorescence of AztC upon zinc binding [24]. This combined with crystal structures of both AztC [24][25] and AztD [26] make this system ideal for detailed mechanistic investigations of direct, protein-to-protein metal transfer as well as zinc binding/dissociation from solution.

Our previous work culminated in a docking model showing the possible transfer complex formed between AztC and AztD (Figure 1). This model highlights several important structural features. First, the flexible loop of AztC that we refer to as the D-Loop projects into the central pore of the AztD beta-propeller structure. This loop and each of its 3 His residues are essential for transfer [25]. Secondly, AztC (residues 222–229) referred to as the Z-loop must be displaced away from the zinc binding site in order for the complex to form. This is true in the apo AztC structure, but this loop closes down over the zinc site in the holo structure. This was suggested to provide a means for dissociation of the complex after transfer. Finally, the 6 N-terminal residues after cleavage of the periplasmic targeting sequence of AztD (residues 22–27) are not

observed in the crystal structure, but would be positioned at the interface with AztC according to the model. Residues 23–29 form a DHDHDHE motif that may bind zinc and/or facilitate transfer to AztC. Zinc binding to this N-terminal motif (NTM) was suggested by the observation of a third, relatively low-affinity binding site in addition to the two high-affinity sites in AztD [23].
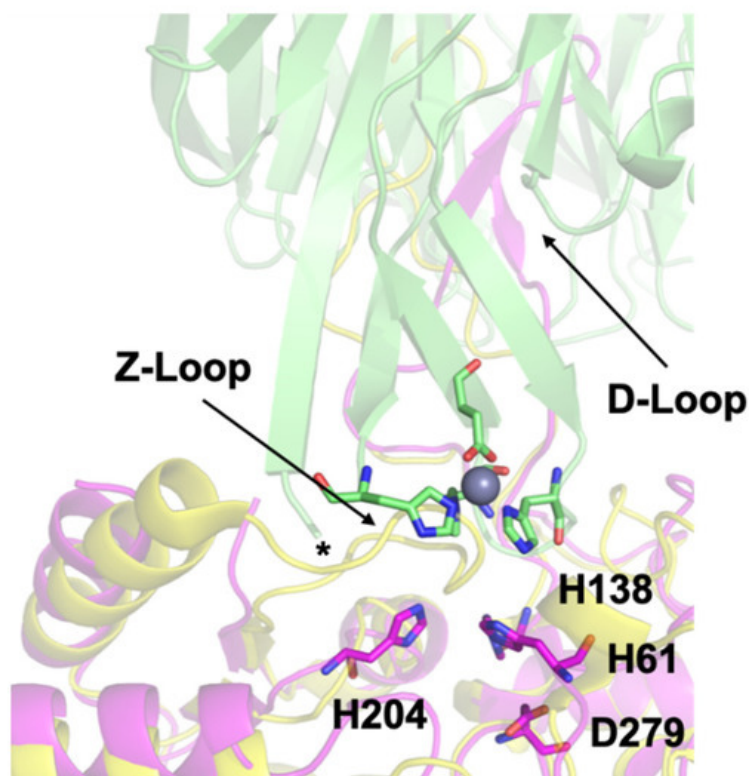

Figure 1. Docking model of the AztC-AztD transfer complex. AztD is shown in green with zinc binding residues shown as sticks colored according to element and zinc as a gray sphere. The first modeled N-terminal residue of AztD (His 28) is indicated by an asterisk. Apo AztC is shown in magenta with zinc binding residues labeled and shown as sticks colored according to element. Holo AztC superimposed on the apo form is shown in yellow, illustrating how the position of the Z-loop in this structure would block zinc transfer.

2. Zinc Dissociation

Apo WT or mutant AztC was diluted to 1 µM in binding buffer in a stirred cuvette at ambient temperature. Protein was titrated with up to 3 equivalents of $ZnCl_2$ and the fluorescence intensity monitored to ensure saturation. Dissociation was initiated by the addition of EDTA to 1.0 mM and the decay in emission intensity at 315 nm was monitored. Data was fit by a single exponential function using DYNAFIT [29][30].

3. Zinc Binding and Transfer by Intrinsic Fluorescence

All fluorescence measurements were made using a Varian Cary Eclipse fluorescence spectrophotometer as previously described. Titration experiments were performed with AztC proteins at 10 µM in binding buffer. These were titrated with $ZnCl_2$ or AztD reconstituted with 2 equivalents of $ZnCl_2$ followed by desalting into binding buffer using Zeba™ spin desalting columns (Pierce Biotechnology™, Rockford, IL, USA). In titrations of apo-AztC with holo-AztD, 5–15 min of equilibration was allowed between measurements. After addition of holo-AztD to 14 µM, 20 µM of $ZnCl_2$ was added to determine AztC saturation.

Kinetic experiments were performed as previously described [26] with minor modifications. Apo AztC at 0.5 µM in binding buffer containing 1 mM EDTA was placed in a stirred cell at ambient temperature. Transfer was initiated by addition of varying concentrations of AztD reconstituted as above but omitting the desalting step. Fluorescence emission at 315 nm (λ_{exc} = 278 nm) was recorded over time. Slit widths were varied to optimize signal to noise and avoid saturation at high protein concentration. First order fits to the data were generated using the onboard Cary Eclipse software. Inhibition experiments were performed similarly to those above but included varying concentrations of H138/204A or ΔD-loop AztC in addition to WT AztC at 0.5 µM. Transfer was initiated by addition of 0.5 µM reconstituted WT AztD and monitored as above.

4. Zinc Binding and Dissociation

The zinc binding affinity of WT AztD, WT AztC, ΔD-Loop AztC, and ΔZ-Loop AztC were previously determined by competition assay with the fluorophore MagFura-2 (MF2) (Table 1). Here we apply this technique to H138/204A AztC and a deletion of the N-terminal motif (residues 23–29) in AztD (ΔNTM AztD) (Figure 2). The former binds approximately one equivalent (0.85) of zinc with a Kd below the detection limit of this assay (≤0.1 nM), making it indistinguishable from WT. ΔNTM AztD binds two equivalents of zinc with very high affinity. Previous work with WT AztD indicated some negative cooperativity between high affinity binding sites. Intriguingly, this appears to be largely eliminated in the ΔNTM mutant. Further, the third binding site in WT AztD is not observed, consistent with relatively low affinity zinc binding by this motif. We also evaluated zinc binding to H138/204A by intrinsic protein fluorescence (Figure 2C,D). Like WT, this mutant exhibits a roughly 2-fold increase in fluorescence emission intensity saturating at one equivalent of added zinc consistent with high affinity binding.
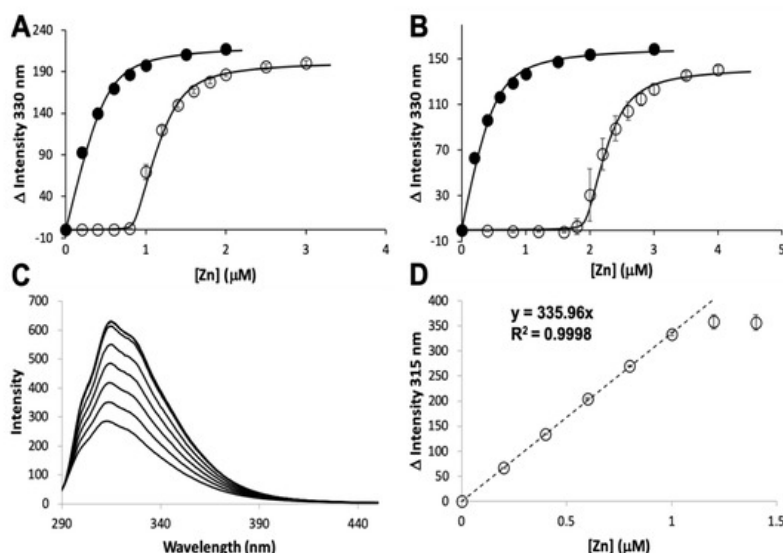

Figure 2. Zinc binding by AztC and AztD mutants. Intensity change of MF2 at 330 nm with increasing zinc in the absence (solid circles) and presence (empty circles) of apo H138/204A AztC (**A**) and ΔN-terminal motif (NTM) AztD (**B**). (**C**) Fluorescence emission spectra of H138/204A AztC (λ_{exc} = 278 nm) and (**D**) magnitude of the fluorescence intensity change with increasing zinc concentration. Titrations containing protein were performed in triplicate and error bars represent the standard deviation between measurements. Least squared fits are shown as solid lines for (**A**) and (**B**) and a dotted line for the linear fit in (**D**) with slope and R^2 values indicated.

Table 1. Zinc binding affinity and stoichiometry of WT and mutant AztD.

Protein	Site	K_d ± S.D. (nM)	k_{off} ± S.D. (min^{-1})	k_T (M^{-1} × s^{-1})
WT AztD [23]	1	0.7 ± 0.3		
	2	54 ± 8		
	3	340 ± 110		
ΔS1 AztD [26]	2	1.3 ± 0.7		
	3	248 ± 81		
ΔS2 AztD [26]	1	0.1 *		
	3	158 ± 35		
ΔNTM AztD	1	0.1 *		1.50 × 10^{-3}
	2	0.2 ± 0.1		
WT AztC [24]	1	0.3 ± 0.1	1.2 ± 0.1 × 10^{-3}	1.33 × 10^{-3} [26]; 1.55 × 10^{-3} (this work)
ΔD-Loop AztC [25]	1	0.2 ± 0.1	0.9 ± 0.1 × 10^{-3}	nd
ΔZ-Loop AztC [25]	1	0.2 *	7.0 ± 0.1 × 10^{-3}	2.92 × 10^{-3}

Protein	Site	$K_d \pm$ S.D. (nM)	$k_{off} \pm$ S.D. (min^{-1})	k_T (M$^{-1} \times$ s^{-1})
H138/204A AztC [24]	1	0.1 *	$623.4 \pm 0.5 \times 10^{-3}$	

The MF2 assay does not reveal any significant differences between the affinities of the various AztC mutants, likely because each Kd is near or below the detection limit. Thus, we developed an intrinsic fluorescence assay to monitor the zinc off-rate for each (Table 1). Briefly, protein is saturated with zinc as determined by fluorescence emission (Figure 3A). Each of the AztC proteins investigated here is similar in terms of the magnitude of fluorescence intensity change upon zinc binding. Next, a large excess of EDTA is added to capture metal as it dissociates, and the decrease in fluorescence intensity is monitored over time as a direct measure of zinc loss. As expected, the zinc off-rates for WT and ΔD-Loop AztC are comparable and extremely slow (Figure 3B,C). However, deletion of the Z-loop causes a more than 5-fold increase in off-rate (Figure 3D), consistent with the function of this feature in closing down over the zinc site. Mutation of the two zinc ligands His138 and His204 causes a dramatic increase in off-rate, approximately 600 times faster than WT (Figure 3E). Assuming an upper limit to the Kd of 0.1 nM as indicated from the MF2 assay, this suggests that zinc binding to this mutant is near the diffusion limit, around 10^8 M$^{-1} \times$ s^{-1}.
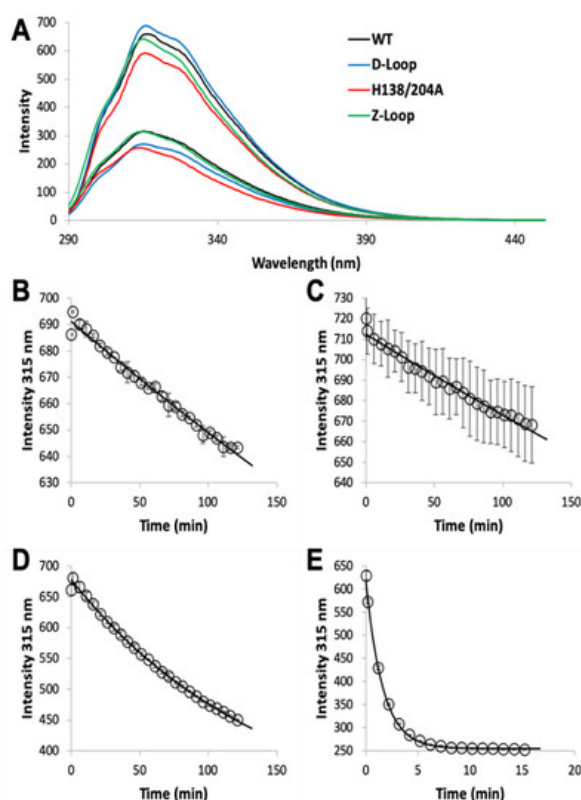

Figure 3. Zinc dissociation from WT and mutant AztC. (**A**) Fluorescence emission spectra of WT (black), ΔD-Loop (blue), ΔZ-Loop (green) and H138/204A (red) AztC before and after addition of saturating ZnCl$_2$. Upon addition of excess EDTA, the emission intensity at 315 nm was tracked over time for WT (**B**), ΔD-Loop (**C**), ΔZ-Loop (**D**), and H138/204A (**E**) AztC. Dissociation experiments were performed in triplicate and error bars represent the standard deviation between measurements.

5. Zinc Transfer from AztD

Transfer of zinc from AztD to AztC can be followed by the increase in AztC fluorescence upon zinc binding [23][25][26]. Previous work indicates that this process requires the presence of the D-Loop, but transfer was still observed to ΔZ-Loop AztC. However, the kinetics were not previously evaluated. Here we demonstrate that the rate of transfer from WT AztD to ΔZ-Loop AztC is increased approximately two-fold relative to WT AztC under the same conditions (Table 1, Figure 4). In contrast, deletion of the NTM from AztD appears to have no effect on the rate of transfer to WT AztC.
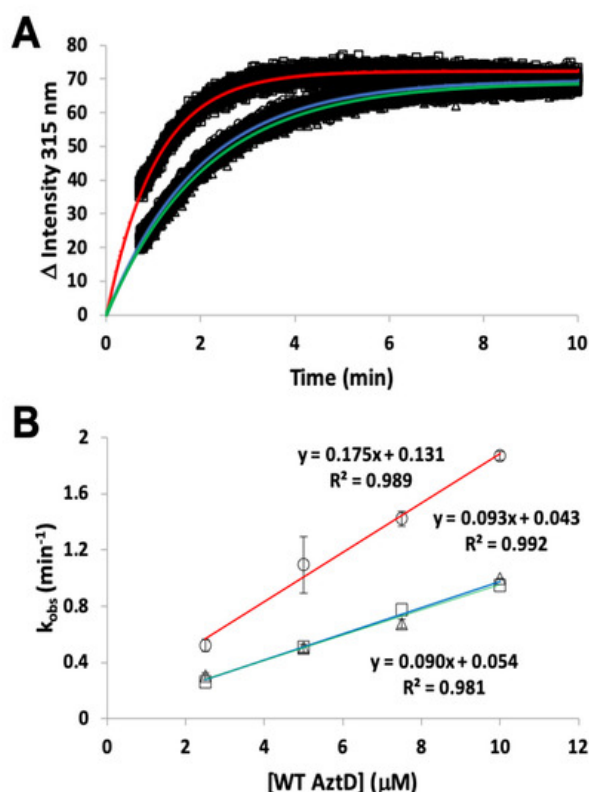
Figure 4. Kinetics of zinc transfer between mutants of AztD and AztC. (**A**) Representative kinetic data from standard fluorescence emission experiments for WT AztD to WT AztC (circles), ΔNTM AztD to WT AztC (triangles), and WT AztD to ΔZ-Loop (squares) with fits to a first order kinetic scheme (blue, green and red, respectively). (**B**) Observed first order rate constant versus AztD concentration for standard fluorescence data under pseudo-first order conditions. Error bars represent standard deviations from duplicate experiments ($n = 2$) except for the WT AztD to WT AztC experiment, which was run a single time to confirm previous data under current conditions. Symbols and linear fit colors are as for (**A**).

The rate of transfer to H138/204A AztC could not be evaluated because of the rapid off-rate of zinc for this mutant. To determine if zinc transfer to this mutant from AztD was possible, it was titrated with holo AztD in the absence of EDTA (Figure 5). Although the fluorescence changes were smaller than for WT, they were nevertheless greater than for ΔD-Loop AztC. These changes also did not reach saturation after 1.4 equivalents of AztD were added and appear to have a roughly hyperbolic rather than linear dependence on AztD concentration. Cumulatively, these data suggest that zinc can be transferred to H138/204A AztC, but the rapid off-rate from this mutant allows an equilibrium to be established between zinc binding to it and AztD. This is in contrast to the virtually unidirectional transfer of zinc to WT AztC, which serves as a kinetic trap for zinc. This also differs from the behavior of ΔD-Loop AztC, which cannot access zinc from AztD at all.
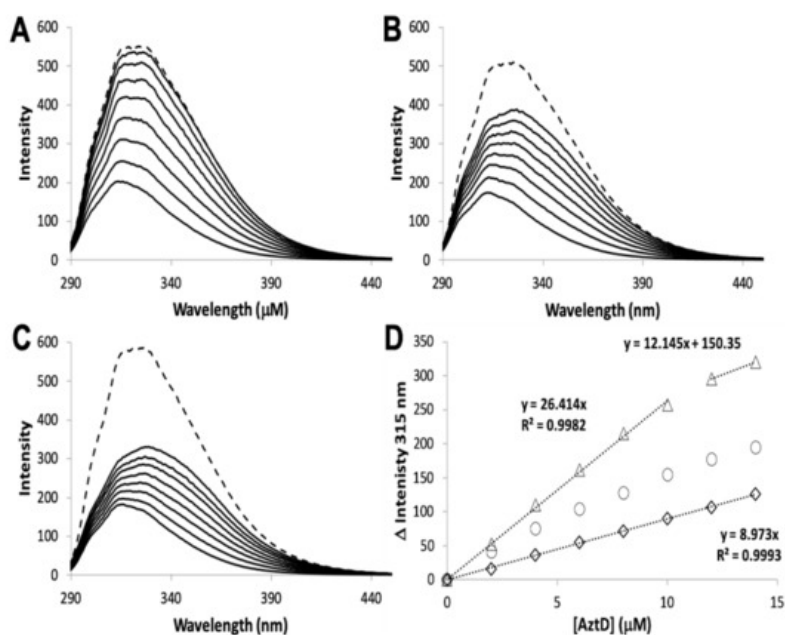
Figure 5. Zinc transfer by intrinsic fluorescence. Reconstituted WT AztD was titrated into apo WT (**A**), H138/204A (**B**), or ΔD-Loop (**C**) AztC. Fluorescence emission spectra (λ_{exc} = 278 nm) were recorded after each addition of AztD and the intensity change at 315 nm plotted as a function of AztD concentration (**D**) with equations for linear fits indicated where appropriate. A saturating concentration of $ZnCl_2$ (1.1 mM) was added after the titration to assess whether transfer from AztD was complete (dotted line, A, B, and C).

References

1. Magistrato, A.; Pavlin, M.; Qasem, Z.; Ruthstein, S. Copper trafficking in eukaryotic systems: current knowledge from e xperimental and computational efforts. Curr. Opin. Struct. Biol. 2019, 58, 26–33, doi:10.1016/j.sbi.2019.05.002.

2. Kambe, T.; Tsuji, T.; Hashimoto, A.; Itsumura, N. The Physiological, Biochemical, and Molecular Roles of Zinc Transport ers in Zinc Homeostasis and Metabolism. Physiol. Rev. 2015, 95, 749–784, doi:10.1152/physrev.00035.2014.

3. Blindauer, C.A. Bacterial metallothioneins: past, present, and questions for the future. JBIC J. Biol. Inorg. Chem. 2011, 16, 1011–1024, doi:10.1007/s00775-011-0790-y.

4. Nairn, B.L.; Lonergan, Z.; Wang, J.; Braymer, J.; Zhang, Y.; Calcutt, M.W.; Lisher, J.P.; Gilston, B.A.; Chazin, W.J.; De Crécy-Lagard, V.; et al. The Response of Acinetobacter baumannii to Zinc Starvation. Cell Host Microbe 2016, 19, 826 –836, doi:10.1016/j.chom.2016.05.007.

5. Chandrangsu, P.; Huang, X.; Gaballa, A.; Helmann, J.D. Bacillus subtilis FolE is sustained by the ZagA zinc metallocha perone and the alarmone ZTP under conditions of zinc deficiency. Mol. Microbiol. 2019, 112, 751–765, doi:10.1111/mm i.14314.

6. Neupane, D.P.; Jacquez, B.; Sundararajan, A.; Ramaraj, T.; Schilkey, F.D.; Yukl, E.T. Zinc-Dependent Transcriptional R egulation in Paracoccus denitrificans. Front. Microbiol. 2017, 8, doi:10.3389/fmicb.2017.00569.

7. Biemans-Oldehinkel, E.; Doeven, M.K.; Poolman, B. ABC transporter architecture and regulatory roles of accessory do mains. FEBS Lett. 2005, 580, 1023–1035, doi:10.1016/j.febslet.2005.11.079.

8. Higgins, C.F. ABC Transporters: From Microorganisms to Man. Annu. Rev. Cell Biol. 1992, 8, 67–113, doi:10.1146/ann urev.cb.08.110192.000435.

9. Berntsson, R.P.-A.; Smits, S.H.J.; Schmitt, L.; Slotboom, D.-J.; Poolman, B. A structural classification of substrate-bindi ng proteins. FEBS Lett. 2010, 584, 2606–2617, doi:10.1016/j.febslet.2010.04.043.

10. Loisel, E.; Jacquamet, L.; Serre, L.; Bauvois, C.; Ferrer, J.L.; Vernet, T.; Di Guilmi, A.M.; Durmort, C. AdcAII, A New Pne umococcal Zn-Binding Protein Homologous with ABC Transporters: Biochemical and Structural Analysis. J. Mol. Biol. 2 008, 381, 594–606, doi:10.1016/j.jmb.2008.05.068.

11. Hood, M.I.; Skaar, E.P. Nutritional immunity: transition metals at the pathogen-host interface. Nat. Rev. Genet. 2012, 1 0, 525–37, doi:10.1038/nrmicro2836.

12. Kehl-Fie, T.E.; Skaar, E.P. Nutritional immunity beyond iron: a role for manganese and zinc. Curr. Opin. Chem. Biol. 20 10, 14, 218–224, doi:10.1016/j.cbpa.2009.11.008.

13. Panina, E.M.; Mironov, A.A.; Gelfand, M.S. Comparative genomics of bacterial zinc regulons: Enhanced ion transport, p athogenesis, and rearrangement of ribosomal proteins. Proc. Natl. Acad. Sci. USA 2003, 100, 9912–9917, doi:10.1073/ pnas.1733691100.

14. Plumptre, C.D.; Eijkelkamp, B.A.; Morey, J.R.; Behr, F.; Couñago, R.M.; Ogunniyi, A.D.; Kobe, B.; O'Mara, M.L.; Paton, J.C.; McDevitt, C.A. AdcA and AdcAII employ distinct zinc acquisition mechanisms and contribute additively to zinc hom eostasis in Streptococcus pneumoniae. Mol. Microbiol. 2014, 91, 834–851, doi:10.1111/mmi.12504.

15. Cao, K.; Li, N.; Wang, H.; Cao, X.; He, J.; Zhang, B.; He, Q.-Y.; Zhang, G.; Sun, X. Two zinc-binding domains in the tra nsporter AdcA from Streptococcus pyogenes facilitate high-affinity binding and fast transport of zinc. J. Biol. Chem. 201 8, 293, 6075–6089, doi:10.1074/jbc.m117.818997.

16. Ilari, A.; Alaleona, F.; Tria, G.; Petrarca, P.; Battistoni, A.; Zamparelli, C.; Verzili, D.; Falconi, M.; Chiancone, E. The Sal monella enterica ZinT structure, zinc affinity and interaction with the high-affinity uptake protein ZnuA provide insight int o the management of periplasmic zinc. Biochim. Biophys. Acta 2014, 1840, 535–544, doi:10.1016/j.bbagen.2013.10.01 0.

17. Petrarca, P.; Ammendola, S.; Pasquali, P.; Battistoni, A. The Zur-Regulated ZinT Protein Is an Auxiliary Component of t he High-Affinity ZnuABC Zinc Transporter That Facilitates Metal Recruitment during Severe Zinc Shortage. J. Bacteriol. 2010, 192, 1553–1564, doi:10.1128/jb.01310-09.

18. Gabbianelli, R.; Scotti, R.; Ammendola, S.; Petrarca, P.; Nicolini, L.; Battistoni, A. Role of ZnuABC and ZinT in Escherichia coli O157:H7 zinc acquisition and interaction with epithelial cells. BMC Microbiol. 2011, 11, 36, doi:10.1186/1471-2180-11-36.

19. Graham, A.I.; Hunt, S.; Stokes, S.L.; Bramall, N.; Bunch, J.; Cox, A.G.; McLeod, C.W.; Poole, R.K.; Oka, M.; Sumita, N.; et al. Severe Zinc Depletion of Escherichia coli. J. Biol. Chem. 2009, 284, 18377–18389, doi:10.1074/jbc.m109.001503.

20. Eijkelkamp, B.A.; Pederick, V.G.; Plumptre, C.D.; Harvey, R.M.; Hughes, C.E.; Paton, J.C.; McDevitt, C.A. The First Histidine Triad Motif of PhtD Is Critical for Zinc Homeostasis in Streptococcus pneumoniae. Infect. Immun. 2015, 84, 407–415, doi:10.1128/iai.01082-15.

21. Ogunniyi, A.D.; Grabowicz, M.; Mahdi, L.K.; Cook, J.; Gordon, D.L.; Sadlon, T.A.; Paton, J.C. Pneumococcal histidine triad proteins are regulated by the Zn 2+ -dependent repressor AdcR and inhibit complement deposition through the recruitment of complement factor H. FASEB J. 2008, 23, 731–738, doi:10.1096/fj.08-119537.

22. Bersch, B.; Bougault, C.; Roux, L.; Favier, A.; Vernet, T.; Durmort, C. New Insights into Histidine Triad Proteins: Solution Structure of a Streptococcus pneumoniae PhtD Domain and Zinc Transfer to AdcAII. PLOS ONE 2013, 8, e81168, doi:10.1371/journal.pone.0081168.

23. Handali, M.; Roychowdhury, H.; Neupane, D.P.; Yukl, E.T. AztD, a Periplasmic Zinc Metallochaperone to an ATP-binding Cassette (ABC) Transporter System in Paracoccus denitrificans. J. Biol. Chem. 2015, 290, 29984–29992, doi:10.1074/jbc.m115.684506.

24. Handali, M.; Neupane, D.P.; Roychowdhury, H.; Yukl, E.T. Transcriptional Regulation, Metal Binding Properties and Structure of Pden1597, an Unusual Zinc Transport Protein from Paracoccus denitrificans. J. Biol. Chem. 2015, 290, 11878–11889, doi:10.1074/jbc.m115.645853.

25. Neupane, D.P.; Avalos, D.; Fullam, S.; Roychowdhury, H.; Yukl, E.T. Mechanisms of zinc binding to the solute-binding protein AztC and transfer from the metallochaperone AztD. J. Biol. Chem. 2017, 292, 17496–17505, doi:10.1074/jbc.M117.804799.

26. Neupane, D.P.; Fullam, S.H.; Chacón, K.N.; Yukl, E.T. Crystal structures of AztD provide mechanistic insights into direct zinc transfer between proteins. Commun. Biol. 2019, 2, 308–12, doi:10.1038/s42003-019-0542-z.

27. Edelhoch, H. Spectroscopic Determination of Tryptophan and Tyrosine in Proteins*. Biochemistry 1967, 6, 1948–1954, doi:10.1021/bi00859a010.

28. Golynskiy, ‡ M.V.; Gunderson, § W.A.; Hendrich, M.P.; Cohen, S.M. Metal Binding Studies and EPR Spectroscopy of the Manganese Transport Regulator MntR†. Biochemistry 2006, 45, 15359–15372, doi:10.1021/bi0607406.

29. Kuzmic, P. Program DYNAFIT for the Analysis of Enzyme Kinetic Data: Application to HIV Proteinase. Anal. Biochem. 1996, 237, 260–273, doi:10.1006/abio.1996.0238.

30. Kuzmic, P. DynaFit—A Software Package for Enzymology. Methods Enzymol. 2009, 467, 247–280, doi:10.1016/s0076-6879(09)67010-5.